WARSAW UNIVERSITY OF TECHNOLOGY Index 351733
FACULTY OF CIVIL ENGINEERING
COMMITTEE FOR CIVIL AND WATER ENGINEERING
POLISH ACADEMY OF SCIENCES ISSN 1230-2945

DOI: 10.24425/ace.2023.147669

ARCHIVES OF CIVIL ENGINEERING

Vol. LXIX ISSUE 4 2023

pp. 445 –457

Research paper

Investigation on cracking performance of UHPC overlaid concrete deck at hogging moment zone of steel-concrete composite girders

Zhiyong Wan[1,2], Guohe Guo[3], Zhiguo Wang[4], Shaohua He[5], Juliang Tan[6], Libo Hou[7]

Abstract: The concrete deck at the negative bending moment region of a continuous steel-concrete composite girder bridge is the weakest part of the structure. Introducing ultra-high performance concrete (UHPC) to the hogging region may overcome the shortage and break through the bottleneck. This paper explores the cracking performance of steel-concrete composite girders with concrete slabs topped by a thin layer of UHPC subjected to a negative bending moment. A real continuous composite girder bridge is briefly introduced as the engineering background, and the cracking characteristic of the concrete deck over the middle piers of the bridge is numerically modeled. Approaches to strengthen the cracking performance of the concrete deck at the hogging region through topping UHPC overlays are proposed. The effectiveness of the approaches is examined by conducting a series of numerical and experimental tests. Numerical results indicate that the normal concrete (NC) deck near the middle forums of the bridge would crack due to the large tensile stress from negative bending moments. Replacing the top concrete with an identical-thick UHPC overlay can increase the cracking resistance of the deck under the moment. As the thickness of the UHPC overlay increased from 6.0 cm to 12.0 cm, the maximum shear stress at the UHPC overlay-to-NC substrate interface under different load combinations was decreased by 56.3%~65.3%. Experimental results show that the first-cracking load of the composite beam using

[1]PhD., College of Civil Engineering, Hunan University, Changsha 410082, China, e-mail: 1095801967@qq.com, ORCID: 0009-0003-6375-9516
[2]Prof. Eng., Guangdong Communication Planning & Design Institute Co., Ltd., Guangzhou 510507, China, e-mail: 1095801967@qq.com, ORCID: 0009-0003-6375-9516
[3]Sen. Eng., Guangdong Yunmao Expressway Co. Ltd., Guangzhou 525346, China, e-mail: 646461088@qq.com, ORCID: 0009-0002-9723-071X
[4]Sen. Eng., Guangdong Yunmao Expressway Co. Ltd., Guangzhou 525346, China, e-mail: 29936966@qq.com, ORCID: 0009-0008-3736-3274
[5]Associate Professor, Guangdong University of Technology, Guangzhou 510006, China, e-mail: hesh@gdut.edu.cn, ORCID: 0000-0002-0727-1976
[6]Sen. Eng., Guangdong Communication Planning & Design Institute Co., Ltd., Guangzhou 510507, China, e-mail: 30119056633@qq.com, ORCID: 0009-0007-6611-9978
[7]Eng., Guangdong Highway Construction Co., LTD, Guangzhou 510623, China, e-mail: 1411853254@qq.com, ORCID: 0009-0000-7293-5444

an NC-UHPC overlaid slab was 2.1 times that using an NC slab. The application of a UHPC overlaid deck can significantly improve the crack performance of the steel-concrete composite girder bridge.

Keywords: steel-concrete composite girder, concrete deck, negative bending moment, ultra-high performance concrete, cracking resistance

1. Introduction

The steel-concrete composite girder bridge, incorporating steel and concrete components as a single union to carry dead and traffic loads, can fully exert the mechanical properties of the materials [1–3]. However, for the composite bridge in a continuous span arrangement, the concrete deck over the middle piers is exposed to a high risk of cracking due to negative bending moments. The cracking of concrete in the area decreases the structural stiffness of the girder, and harmful ions penetrating the cracks corrode steel reinforcements in the concrete and shear connectors at the steel beam-to-concrete decks, decreasing the serviceability and durability of the structure [4, 5].

Engineers have tried to improve the cracking performance of concrete decks in continuous steel-concrete composite girder bridges. Many strengthening approaches, such as applying temporary counterweight at the middle span, optimizing concrete slab fabrication sequence, involving prestressed tendons in concrete slabs, and rising-falling supports over middle piers, have been used in engineering practices. For example, based on the configuration of a steel-concrete composite girder that belonged to the Hong Kong-Zhuhai-Macao Bridge, Liu et al. [6] examined the effectiveness of using prestressed tendons and rising-falling middle support methods to increase the cracking resistance of the concrete decks under negative bending moment. Their experimental and numerical results indicate that the maximum tensile stress in the concrete decks was decreased by employing the approaches, and a practical lifting height for the middle supports was suggested for the bridge.

Similar to the compressions from prestressed tendons used at the hogging moment region, uplifting middle fulcrums before casting concrete and lowering the fulcrums after completing the girder generates compressive stress in concrete. However, due to the synergistic effects between the steel beam and concrete slab, the efficiency of using prestressed tendons resisting concrete tensile stress is comparatively low. The development of concrete shrinkage and creep also reduces the compressive stress from the steel strands [7–9]. The positional shift of middle fulcrums is also difficult to be realized at the site. Optimizing the concrete slab fabrication sequence and applying a temporary counterweight at a positive bending moment region during construction is more practical for the composite girder. Installing concrete slabs at the middle span before that near the fulcrums can minimize the negative bending moment from structural self-weight. Removing the counterweight also brings additional compression to the concrete at the hogging region [10–14].

Recently, another potential approach involving ultra-high performance concrete (UHPC) in the hogging moment region has been proposed for deck strengthening [15]. The UHPC is a cement-based composite material with super high strength and advanced durability, which can well overcome the shortage of normal concrete decks with weak tensile

performance under hogging moments [16, 17]. According to the experimental results from orthotropic steel decks with UHPC overlays conducted by Zhou et al. [18], the tensile stress at the first cracking of the UHPC deck reached up to 10.79 MPa, and the ultimate resistance of the deck was 14 times that of the normal concrete deck. The UHPC deck possesses good cracking resistance and is suitable for resisting the tensile stress in the negative bending moment region of continuous steel-concrete composite girder bridges [19].

Unfortunately, the price of commercial UHPC products is very high, and replacing the entire concrete with UHPC for bridge construction is impractical. An economical way is to replace the top layer of normal concrete at the hogging region with a thin layer of UHPC and retain the normal concrete substrate to reduce costs [20]. Accordingly, this paper investigates the cracking performance of steel-concrete composite girders with normal concrete slabs topped by a thin layer of UHPC at the negative bending moment region. A real continuous composite girder is selected as the background, and its cracking characteristic is numerically simulated. The effectiveness of the UHPC overlay strengthening approach is examined by conducting a series of numerical and experimental tests. The study's outcome provides a reference for improving concrete decks in composite bridges.

2. Engineering background

2.1. Information on prototype bridge

The prototype bridge is a continuous steel-concrete composite girder part of the Yunmao Expressway in the Guangdong Province of China. As shown in Fig. 1, the total length, deck width, and cross-section depth of the bridge were 160 m (4×40 m), 12.5 m, and 2.16 m,

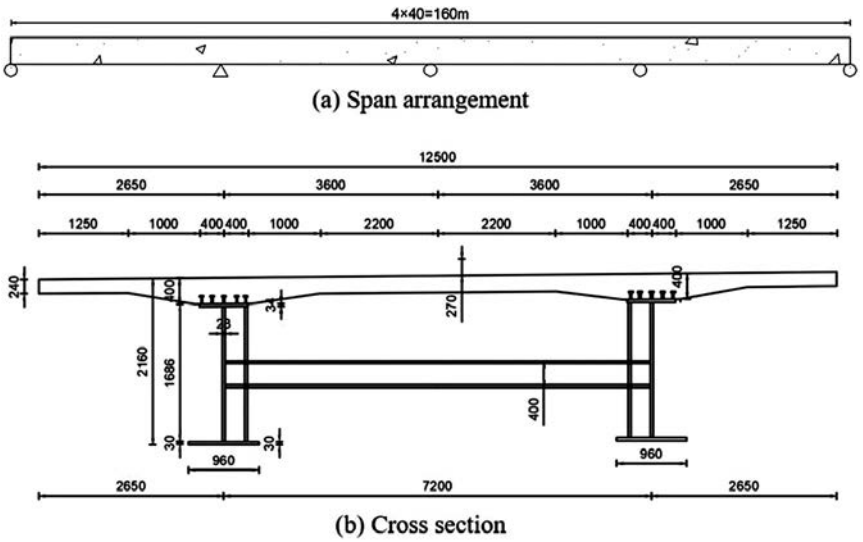

Fig. 1. Arrangement and configuration of prototype bridge (mm)

respectively. The concrete deck was fabricated using C55 normal concrete (with a nominal compressive strength of 55.0 MPa), and the steel beam was welded through cutting C345C grade steel profiles (with a nominal yield strength of 345.0 MPa). The thickness of the concrete deck near the steel web and longitudinal axis was 40 cm and 26 cm, respectively. The steel beams in parallel arrangement had an interval distance of 670 cm, a top flange thickness of 3.6 cm, a bottom flange thickness of 5.4 cm, and a web thickness of 2.8 cm. The width of the top and bottom steel flanges were 90 cm and 130 cm, respectively. Headed steel studs with a shank diameter and length of 13 mm and 100 mm, respectively were equipped at the interface between the top steel flange and concrete decks to ensure the integrality of the composite girder. The design vehicle speed and seismic peak acceleration of the bridge were 100 km/h and 0.05 g, respectively.

2.2. Cracking performance assessment

The cracking performance of the concrete deck at the negative bending moment region of the prototype bridge is assessed by the finite element (FE) models. Fig. 2 shows the model established using ANSYS 15.0 agency. In the model, the Solid 65 elements with eight nodes are used to simulate the cracking, crushing, and stress-releasing characteristics of the concrete slabs, and the Shell 63 elements with four nodes are used to simulate the elastic behavior of the steel beams. The concrete deck and steel beam elements are 50 mm and 25 mm, respectively. Considering that the actual number of shear connectors in the

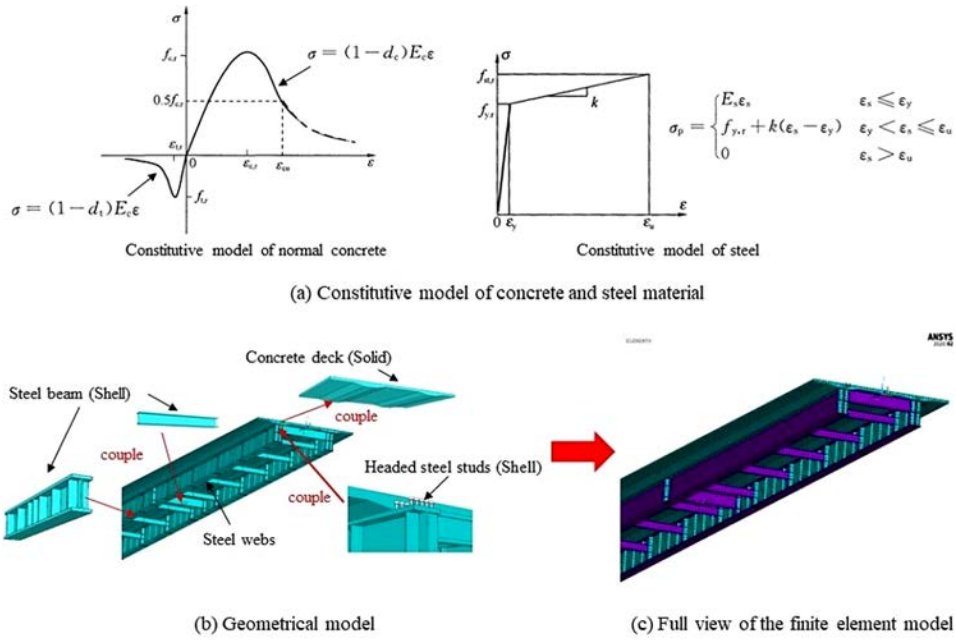

Fig. 2. Finite element model for the selected bridge

bridge is far beyond the required number of the connectors for eliminating potential failure of the connectors at the ultimate state of the girder, all nodes at the concrete deck to the steel beam interface are coupled together. No relative slip would occur to the steel-concrete contacting surfaces in the model. The constitutive model of the concrete is defined based on the stress-strain relationship provided in the Chinese code GB 50010-2010 [21], and the bilinear Kinematic Hardening Plasticity constitutive model was used for all steel members.

In order to evaluate the cracking performance of the concrete deck under critical loads, load combinations of the temporary ultimate, standard, and short-term that are defined in Chinese code [19] are applied to the models. The stress results for concrete decks over middle piers produced by the FE model are summarized in Fig. 3. The asymmetrically distributed concrete stress is due to the influence of the traffic loads. As shown in Fig. 3a, under the temporary ultimate load combination, the maximum tensile stress in the concrete deck is 3.5 MPa. On the other hand, Figs. 3b and 3c show that the maximum tensile stress of the concrete under the standard and short-term load combinations reaches approximately 8.0 MPa, and the concrete tensile stress near the middle fulcrums is mostly between 4.0 MPa and 8.0 MPa. The concrete tensile stress at the negative bending moment region of the bridge is far beyond the allowable strength of the C55 concrete, indicating that the deck at the region would crack after the completion of the bridge. From the perspective of guaranteeing structure durability, improving the cracking resistance of the concrete decks at the hogging region of the prototype bridge is critical.

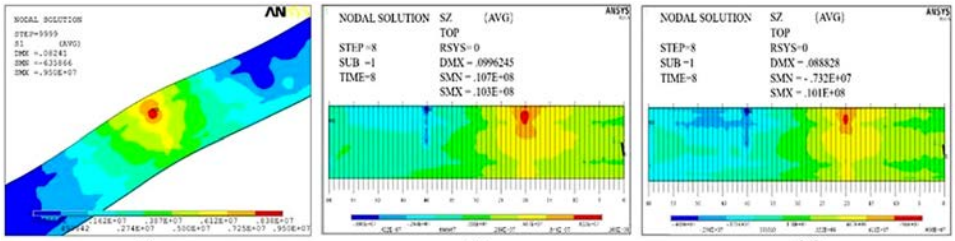

Fig. 3. Stresses in concrete slabs at negative moment region: a) temporary ultimate load combination, b) Standard load combination, c) Short-term load combination (MPa)

3. Methods and feasibility analyses

3.1. NC-UHPC overlaid slab

As indicated by the above analysis, the maximum tensile stress of 8.0 MPa is larger than the allowable tensile strength of normal concrete but lower than that of the UHPC material. Like the metals subjected to tension, the UHPC owns typical tensile strain-hardening characteristics with the stress increases, and the ultimate tensile strain of UHPC can go up to 0.2%, which is 20 times that of the normal concrete. Accordingly, replacing the concrete top layer at the negative bending moment region with a UHPC overlay is reasonable to

prevent decks from cracking. According to the replacement ratio of the UHPC overlay, three types of concrete decks, including the NC-UHPC overlaid deck (with a UHPC replacement ratio of 30% and 60%, respectively) and the pure UHPC deck (with a UHPC replacement ratio of 100%), are developed for the prototype bridge. The replacement ratio is the value of the UHPC sectional area divided by the entire cross-sectional area of the deck. Table 1 presents the details of the overlaid decks. The baseline pure NC deck is also listed in the table for easy comparison.

Table 1. Information of NC-UHPC overlaid deck

Group	Description	UHPC thickness (cm)	NC thickness (cm)	UHPC replacement ratio
NN	Pure NC deck	0	20	0%
NU1	NC-UHPC overlaid deck	6	14	30%
NU2	NC-UHPC overlaid deck	12	8	60%
UU	Pure UHPC deck	20	0	100%

In order to examine the cracking performance of the composite girders using the proposed NC-UHPC overlaid decks, reduced-scale steel-concrete composite beams mimicking the configurations and dimensions of the aforementioned bridge are designed for numerical analysis. Fig. 4 presents the configuration and arrangement of steel-concrete composite beams with the specified concrete decks. The total length, deck width, and sectional depth of the composite beam are 420 cm, 120 cm, and 68 cm, respectively. The width and thickness of the top and bottom steel flanges are 40 cm and 3.6 cm, respectively. The arrangement of shear connectors at the steel-to-concrete interface and steel reinforcements in concrete decks are identical to the background bridge.

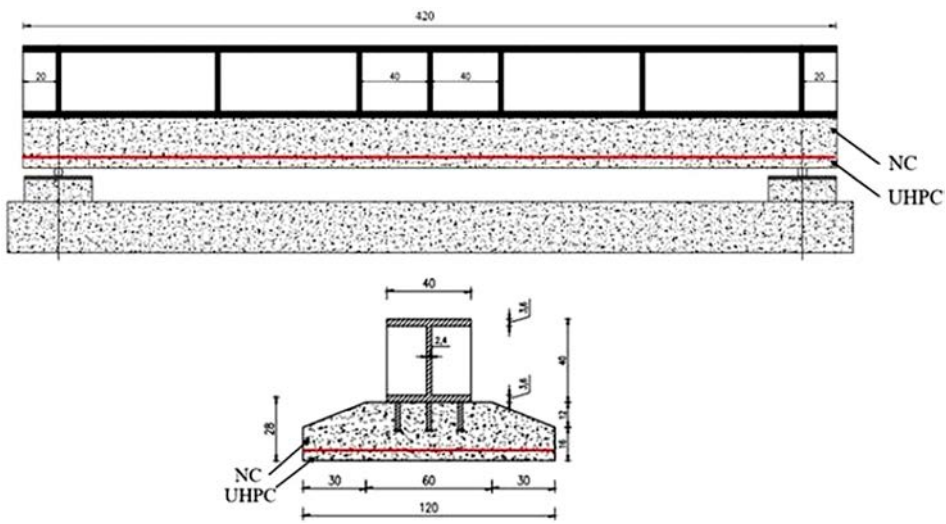

Fig. 4. Composite beams with specified concrete decks (cm)

3.2. Modeling of composite beams with NC-UHPC overlaid slab

The composite beam using NC-UHPC overlaid slab is simulated by the Abaqus software, and the established models are shown in Fig. 5. The steel beam and concrete slab are modeled using the 3-D 8-node reduced integration element C3D8R. The linear truss element T3D2 is used to model the steel reinforcements embedded in the concrete. A 20 mm mesh size was selected for the concrete slab following a separate study to examine convergence. The constitutive models of the steel and normal concrete are the same to those presented in Fig. 2. The constitutive functions given in French code [22] and Zhang [23] are adopted for the UHPC, as presented in Fig. 5. The composite beam is inversely positioned and supported by the two ends. The concentrated load is downward applied to the mid-span point of the beam to produce a negative bending moment of 52.0 kN·m under standard load combination, 159 kN·m under short-term load combination, and 192 kN·m under fundamental load combination. The applied bending moments generate identical concrete stresses to that of the background bridge under specified load combinations.

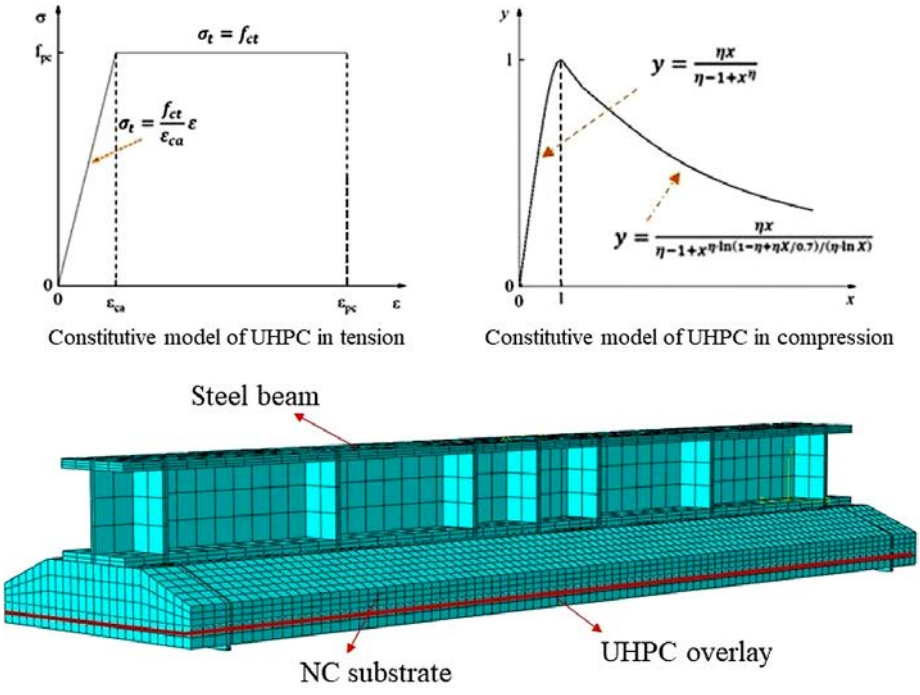

Fig. 5. FE model of composite beams

For the concrete deck, the elasticity modulus, Poisson's ratio, and thermal expansion coefficient of the NC are 34.5 GPa, 0.2, and 1.0×10^{-5}, respectively. The cubic compressive strength, cylinder compressive strength, and tensile strength of the NC material are 55.0 MPa, 35.5 MPa, and 2.74 MPa, respectively. For the UHPC overlay, the elasticity modulus, Poisson's ratio, and thermal expansion coefficient of the NC substates are 43.0 GPa,

0.2, and 1.0×10^{-5}, respectively. The compressive strength, elastic tensile strength, and ultimate tensile strength of the UHPC are 120 MPa, 7.0 MPa, and 10.0 MPa, respectively. The steel beam is made of a Q345C grade steel profile, of which the elasticity modulus, Poisson's ratio, and thermal expansion coefficient are 206 GPa, 0.31, and 1.2×10^{-5}, respectively. The steel beam and concrete deck is fastened together to prevent any slip at the interface. Shrinkage effects of concrete materials are not considered in the established FE models.

3.3. Discussion on simulating results

Figure 6 shows the numerically predicted stress distributions for the beam models under the standard load combination, together with the stresses at critical points of the concrete decks subtracted from the stress nephogram. As can be seen, the maximum concrete tensile stress occurred at the deck bottom of model NN, NU1, NU2, and UU is 2.4 MPa, 2.7 MPa, 2.6 MPa, and 2.7 MPa, respectively. For the composite beam models with an NC-UHPC overlaid deck, the stress at the UHPC overlay-to-NC substrate interface of NU1 and NU2 is 1.5 MPa and 0.51 MPa, respectively. The maximum stress in the concrete decks is below the allowable material strength of NC and UHPC. The composite girder using the decks would not crack under the standard load combination.

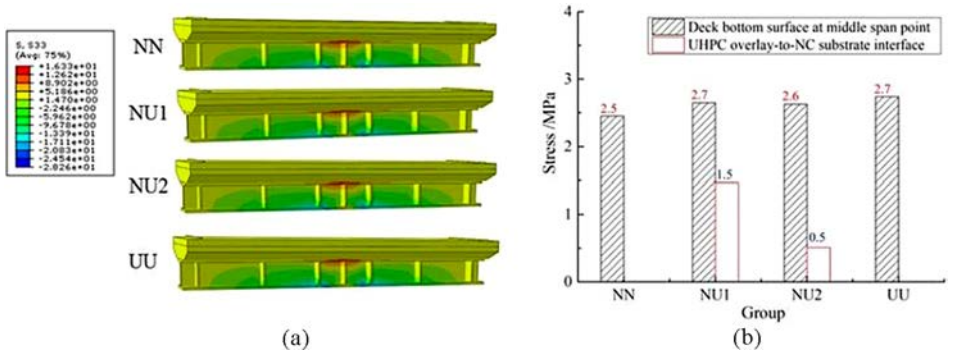

Fig. 6. Stresses of composite beams subjected to standard load combination: a) stress distribution, b) stresses at critical points

The stress distribution of the composite beams under short-term load combination is summarized in Fig. 7. As can be seen, the maximum concrete tensile stress occurred at the deck bottom of model NN, NU1, NU2, and UU is 7.5 MPa, 8.7 MPa, 8.4 MPa, and 8.2 MPa, respectively. The maximum tensile stress of NN is far beyond the tensile strength of the C55 concrete, indicating that concrete cracking would happen to the deck of the NN. In comparison, the tensile strength of UHPC is 10.0 MPa, which is higher than the concrete stresses, and no crack would happen to the UHPC overlay. Concerning the stresses at NC-UHPC overlaid interface, the stress at the UHPC overlay-to-NC substrate interface of NU1 and NU2 is 6.5 MPa and 2.4 MPa, respectively. The large interfacial stress of NU1

indicates that cracking would happen to the overlay-to-substrate contacting surface, despite the retained UHPC overlay under the negative bending moment. Stress results indicate that the concrete decks in groups NU2 and UU possess good cracking performance under the short-term load combination.

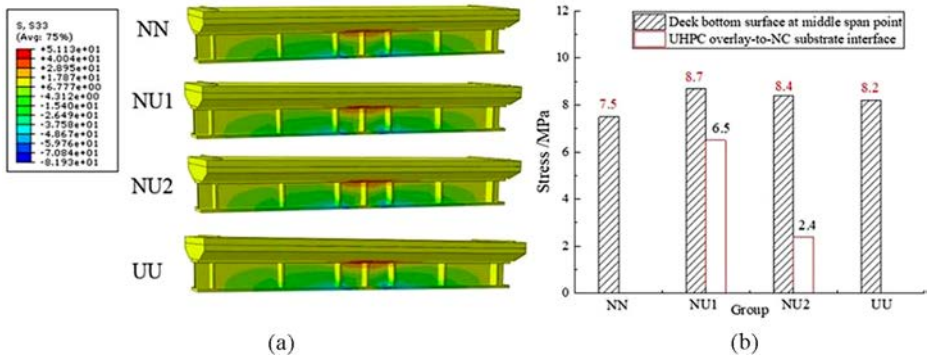

Fig. 7. Stresses of composite beams subjected to short-term load combination: a) stress distribution, b) stresses at critical points

Stress results of the composite beams under fundamental load combination are presented in Fig. 8. Under the temporary ultimate limit status, the maximum tensile stresses in the concrete decks of groups NN, NU1, NU2, and UU is 9.0 MPa, 10.1 MPa, 10.0 MPa, and 9.7 MPa, respectively. Similar to the composite beams subjected to the short-term load combination, concrete decks in the NN model would seriously crack due to the large tensile stress. In comparison, the high tensile strength of UHPC allows the UHPC overlaid decks to remain intact under the ultimate loads. Figure 8 also shows that the stress at the UHPC overlay-to-NC substrate interface of NU1 and NU2 is 7.4 MPa and 3.2 MPa, respectively. The immense stress of NU1 indicates that cracking would happen to the contact surface. The concrete decks in groups NU2 and UU possess good cracking performance under the fundamental load combination.

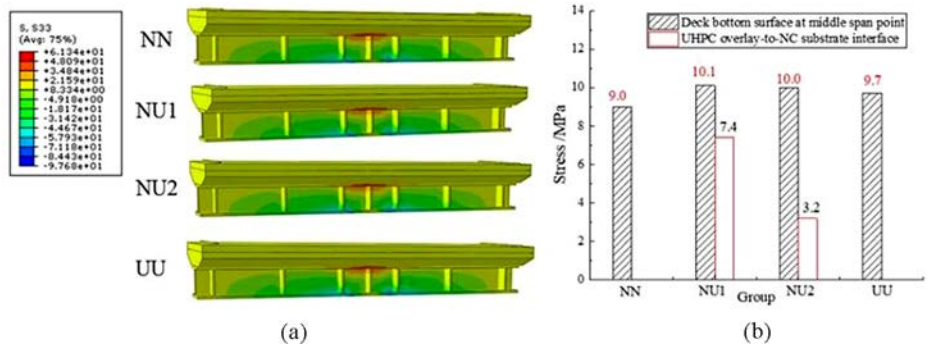

Fig. 8. Stresses of composite beams subjected to fundamental load combination: a) stress distribution, b) stresses at critical points

4. Experimental verifications

In order to verify the cracking resistance of the NC-UHPC overlaid deck, the steel-concrete composite beams of group NN and NU2 were fabricated and tested. The steel beam and head steel studs were fabricated in a factory and then delivered to the laboratory. The steel beams were placed on flat ground and supported by wood frame. Before the normal concrete cast, the steel reinforcements and wood formworks were fabricated, and the UHPC was poured after the hardening of the NC substrates. The UHPC material used for the beam specimens is a commercial product with a target compressive strength of 120 MPa. Table 2 shows the mix proportion of the UHPC. Several short steel rebars with a arrangement interval space of 20 cm were vertically inserted into the NC substrates to strengthen the UHPC-NC interface for the NU2.

Table 2. Mix proportion of UHPC

Cement	Silica fume	Lime	Quartz sand	Superplasticizer	Steel fiber (volume fraction)
1.0	0.25	0.1	1.1	0.03	2.0%

The inversely positioned composite beam specimens were loaded through a hydraulic jack with a maximum loading capacity of 4000 kN. The compressive strength and elasticity of the UHPC measured from the test were 124 MPa and 44.2 GPa, respectively; the corresponding mechanical properties of the normal concrete were 58.6 MPa and 36.5 GPa, respectively. The yield strength, ultimate strength, and elasticity of the steel plate were 412 MPa, 536 MPa, and 206 GPa, respectively. The arrangement of the three-point bending test is shown in Fig. 9.

Fig. 9. Composite beam tests

Table 3 presents the critical loads for evaluating the cracking performance of the deck obtained from composite beam tests and numerical simulation models. As can be seen, results produced by the experimental and numerical work are quiet similar, and the experimentally obtained first cracking load of the NU2 was increased by 208% compared to that of the NN. It should be pointed out that the cracking in NU2 first occurred at the NC-UHPC interface, while that of the NN appeared on the bottom surface of the concrete slab. Concerning the load associated with the first bottom surface crack, the

NU2 exhibited a 4.7 times higher load than the NN, indicating that the UHPC overlay significantly increased the cracking performance of the overlaid deck.

Table 3. Numerical model results and beam test results

Group	Description	Experimental results (kN)		Modeling results (kN)	
		Cracking load of NC	Cracking load of UHPC	Cracking load of NC	Cracking load of UHPC
NN	Pure NC deck	130	–	124	–
NU2	NC-UHPC overlaid deck	412	622	393	595

5. Conclusions

This paper explores the cracking performance of steel-concrete composite girders with concrete slabs topped by a thin layer of UHPC subjected to a negative bending moment. Approaches to strengthen the cracking performance of the concrete deck at the hogging region through topping UHPC overlays are proposed and examined by numerical and experimental results. The main conclusion from the study is drawn as followings:

1. The concrete tensile stress at the negative bending moment region of the selected continuous steel-concrete composite girder is far beyond the allowable strength of the concrete. Improving the cracking resistance of the concrete decks at the hogging region of the prototype bridge is essential.
2. Replacing the top layer of concrete with a UHPC overlay for the negative bending moment region is reasonable to prevent decks from cracking, and the maximum stress in the overlaid concrete deck is below the material allowable strength under the standard load combination of the bridge.
3. The UHPC overlay effectively delayed the surface cracking of the deck. Still, attention should be paid to the overlay-to-substrate interface due to the possible cracking of NC substrates near the overlay. The first cracking load of the NU2 was 2.08 times higher than that of the NN, and the load associated with the first bottom surface cracking of NU2 was 4.7 times that of the NN.

Acknowledgements

The authors express their sincere gratitude for the financial support provided by the Guangdong Basic and Applied Basic Research Foundation (Grant # 2023A1515010535).

References

[1] S. He, Q. Li, G. Yang, X. Zhou, and A.S. Mosallam, “Experimental study on flexural performance of HSS-UHPC composite beams with perfobond strip connectors”, *Journal of Structural Engineering*, vol. 148, no. 6, 2022, doi: 10.1061/(asce)st.1943-541x.0003366.

[2] P. Szewczyk and M. Szumigała, "Optimal design of steel–concrete composite beams strengthened under load", *Materials*, vol. 14, no. 16, 2021, doi: 10.3390/ma14164715.

[3] D. Kisała and K. Furtak, "Comparison of the bending strength of a steel plate–concrete composite beams defined experimentally, theoretically and numerically", *Archives of Civil Engineering*, vol. 66, no. 3, pp. 623–641, 2020, doi: 10.24425/ace.2020.134417.

[4] Z. Fang, et al., "Shear performance of high-strength friction-grip bolted shear connector in prefabricated steel–UHPC composite beams: Finite element modelling and parametric study", *Case Studies in Construction Materials*, vol. 18, 2023, doi: 10.1016/j.cscm.2023.e01860.

[5] S. He, et al., "Structural performance of perforated steel plate-CFST arch feet in concrete girder-steel arch composite bridges", *Journal of Constructional Steel Research*, vol. 201, art. no. 107742, 2023, doi: 10.1016/j.jcsr.2022.107742.

[6] M. Liu, et al., "Pulling force analysis of shear studs in steel-concrete composite continuous box girder of Hongkong-Zhuhai-Macau bridge", *Journal of Wuhan University of Techonology*, vol. 35, no. 2, pp. 118–123, 2013, doi: 10.3963/j.issn.1671-4431.2013.02.023.

[7] L. Dezi, et al., "Construction sequence modelling of continuous steel-concrete composite bridge decks", *Steel and Composite Structures*, vol. 6, no. 2, pp. 123–138, 2006, doi: 10.12989/scs.2006.6.2.123.

[8] F. Gara, G. Leoni, and L. Dezi, "Slab cracking control in continuous steel-concrete bridge decks", *Journal of Bridge Engineering*, vol. 18, no. 12, pp. 1319–1327, 2013, doi: 10.1061/(asce)be.1943-5592.0000459.

[9] P. Men, J. Di, F. Qin, and Y. Su, "Experimental investigation of the shear behavior of slender continuous steel–concrete composite girders in hogging moment", *Journal of Structural Engineering*, vol. 149, no. 1, 2023, doi: 10.1061/jsendh.steng-11537.

[10] Y. Wang, et al., "Experimental study on assembled monolithic steel-prestressed concrete composite beam in negative moment", *Journal of Constructional Steel Research*, vol. 167, art. no. 105667, 2020, doi: 10.1016/j.jcsr.2019.06.004.

[11] El-Zohairy, et al., "Experimental and FE parametric study on continuous steel-concrete composite beams strengthened with CFRP laminates", *Construction and Building Materials*, vol. 157, pp. 885–898, 2017, doi: 10.1016/j.conbuildmat.2017.09.148.

[12] Y. Xu, et al., "Shear behavior of flexible-sleeve perfobond strip connectors: experimental and analytical studies", *Engineering Structures*, vol. 264, art. no. 114380, 2022.

[13] J. Nie, J. Fan, and C.S. Cai, "Stiffness and deflection of steel–concrete composite beams under negative bending", *Journal of Structural Engineering*, vol. 130, no. 11, pp. 1842–1851, 2004, doi: 10.1061/(asce)0733-9445(2004)130:11(1842).

[14] M. Fragiacomo, C. Amadio, and L. Macorini, "Finite-element model for collapse and long-term analysis of steel–concrete composite beams", *Journal of Structural Engineering*, vol. 130, no. 3, pp. 489–497, 2004, doi: 10.1061/(asce)0733-9445(2004)130:3(489).

[15] S. He, et al., "Evaluation of shear lag effect in HSS-UHPC composite beams with perfobond strip connectors: experimental and numerical studies", *Journal of Constructional Steel Research*, vol. 194, art. no. 107312, 2022, doi: 10.1016/j.jcsr.2022.107312.

[16] H. Huang, X. Gao, and L. Teng, "Fiber alignment and its effect on mechanical properties of UHPC: an overview", *Construction and Building Materials*, vol. 296, 2021, doi: 10.1016/j.conbuildmat.2021.123741.

[17] Shafieifar, et al., "Experimental and numerical study on mechanical properties of Ultra High Performance Concrete (UHPC)", *Construction and Building Materials*, vol. 156, pp. 402–411, 2017, doi: 10.1016/j.conbuildmat.2017.08.170.

[18] S. Zhou, et al., "Application of ultra-high performance concrete pavement system to steel bridge deck", *Bridge Construction*, vol. 49, no. S1, pp. 20–25, 2019.

[19] Z. Wan, et al., "Structural performance of steel–concrete composite beams with UHPC overlays under hogging moment", *Engineering Structures*, vol. 270, art. no. 114866, 2022, doi: 10.1016/j.engstruct.2022.114866.

[20] P.R. Prem, and A.R. Murthy, "Acoustic emission and flexural behaviour of RC beams strengthened with UHPC overlay", *Construction and Building Materials*, vol. 123, pp. 481–492, 2016, doi: 10.1016/j.conbuildmat. 2016.07.033.

[21] Ministry of Housing and Urban-Rural Development of the People 's Republic of China, *Code for design of concrete structures*. China Building Industry Press, 2015.

[22] BSI, *Part 5: Code of practice for the design of composite bridges. BS 5400 steel, concrete and composite bridges*. London: British Standards Institution, 1979.

[23] Z. Zhang, et al., "Axial tensile behavior test of ultra high performance concrete", *China Journal of Highway and Transport*, vol. 28, no. 8, pp. 50–58, 2015, doi: 10.3969/j.issn.1001-7372.2015.08.007.

Received: 2023-05-09, Revised: 2023-07-18